

Role of colliding geometry on the balance energy of mass asymmetric systems.

Supriya Goyal*

Department of Physics, Panjab University,
Chandigarh -160 014, India

(Dated: December 6, 2018)

We study the role of colliding geometry on the balance energy (E_{bal}) of mass-asymmetric systems by varying the mass asymmetry ($\eta = A_T - A_P / A_T + A_P$; where A_T and A_P are the masses of the target and projectile, respectively) from 0.1 to 0.7, over the mass range 40-240 and on the mass dependence of the balance energy. Our findings reveal that colliding geometry has a significant effect on the E_{bal} of asymmetric systems. We find that, as we go from central collisions to peripheral ones, the effect of mass asymmetry on E_{bal} increases throughout the mass range. Interestingly, we find that for every fixed system mass (A_{TOT}), the effect of the impact parameter variation is almost uniform throughout the mass-asymmetry range. For each η , E_{bal} follows a power-law behavior ($\propto A^\gamma$) at all colliding geometries.

PACS numbers: 25.70.Pq, 24.10.Lx

In the intermediate energy region (i.e., from 10 MeV/nucleon to 1 GeV/nucleon), there are two major interactions that dominate the nuclear reaction: (i) the attractive nuclear mean field and (ii) the repulsive nucleon-nucleon (nn) interaction. Among the various phenomena observed in this energy region, collective transverse flow is one of the most sensitive and sought-after and has been extensively used over the past three decades to provide information about the nuclear equation of state (EOS) and nn cross section [1–3]. The collective transverse flow is the sideward deflection of the reaction products in phase space and is due to the interactions inside the reaction zone. At low beam energies, the collective transverse flow is dominated by an attractive interaction and the flow is expected to be negative. At high beam energies, the flow is dominated by nn repulsive interactions and the flow is expected to be positive. At a beam energy where the repulsive nn interactions balance the attractive nuclear mean-field interactions, the collective transverse flow disappears. The beam energy at which transverse flow disappears is termed the *balance energy* (E_{bal}) [4].

The balance energy is found to be highly sensitive toward the nuclear matter equation of state, the nn cross section [1–3], the size of the system [5], the asymmetry of the reaction [6], the incident energy of the projectile [7], and the colliding geometry (i.e., the impact parameter) [8].

The importance of the role of system mass [9–11] and colliding geometry [12–15] in the determination of the E_{bal} has been recognized several times in the literature. For the central collisions, the balance energy is found to vary as $A_{TOT}^{-1/3}$ (where A_{TOT} is the total mass of the target and projectile), both experimentally as well as theoretically [9]. Owing to the decrease in the compression

reached in heavy-ion collisions with increase in the impact parameter, E_{bal} is found to increase approximately linearly as a function of impact parameter [13, 14]. It is noted that the role of the impact parameter on the disappearance of flow and on its mass dependence has been studied mainly for symmetric reacting nuclei. However, in a recent study [6], we confronted for the first time the effect of mass asymmetry (η) on E_{bal} using a quantum molecular dynamics (QMD) model [16], but the study was limited to central collisions only ($b/b_{max} = 0.25$). We found that for central collisions, almost independent of the system mass, a uniform effect of mass asymmetry can be seen at the balance energy. Here we aim to extend the study by looking for the effect of colliding geometries on the E_{bal} of mass-asymmetric systems by varying the impact parameter from central to peripheral values. This study is performed with the QMD model explained in Ref. [16].

For the present study, we simulated 1000-5000 events of various reactions in the incident energy range between 90 and 600 MeV/nucleon. In particular, we simulated the reactions of ${}^1_8O + {}^{23}_{11}Na$ ($\eta = 0.1$), ${}^{14}_7N + {}^{26}_{12}Mg$ ($\eta = 0.3$), ${}^{10}_5B + {}^{30}_{14}Si$ ($\eta = 0.5$), and ${}^6_3Li + {}^{34}_{16}S$ ($\eta = 0.7$) for $A_{TOT} = 40$; ${}^{36}_{18}Ar + {}^{44}_{20}Ca$ ($\eta = 0.1$), ${}^{28}_{14}Si + {}^{52}_{24}Cr$ ($\eta = 0.3$), ${}^{20}_{10}Ne + {}^{60}_{28}Ni$ ($\eta = 0.5$), and ${}^{10}_5B + {}^{70}_{32}Ge$ ($\eta = 0.7$) for $A_{TOT} = 80$; ${}^{70}_{32}Ge + {}^{90}_{40}Zr$ ($\eta = 0.1$), ${}^{54}_{26}Fe + {}^{106}_{48}Cd$ ($\eta = 0.3$), ${}^{40}_{20}Ca + {}^{120}_{52}Te$ ($\eta = 0.5$), and ${}^{24}_{12}Mg + {}^{136}_{58}Ce$ ($\eta = 0.7$) for $A_{TOT} = 160$; and ${}^{108}_{48}Cd + {}^{132}_{56}Ba$ ($\eta = 0.1$), ${}^{84}_{38}Sr + {}^{156}_{66}Dy$ ($\eta = 0.3$), ${}^{60}_{28}Ni + {}^{180}_{74}W$ ($\eta = 0.5$), and ${}^{36}_{18}Ar + {}^{204}_{82}Pb$ ($\eta = 0.7$) for $A_{TOT} = 240$. The present study is performed for three values of reduced impact parameter (i.e., $b/b_{max} = 0.25, 0.5, \text{ and } 0.75$). The charges are chosen in such a way that colliding nuclei are stable nuclides; therefore, slight variation in the charges can be seen. Here η is varied from 0.1 to 0.7, keeping A_{TOT} fixed. The values of A_{TOT} vary from 40 to 240. A momentum-dependent soft equation of state with standard energy-dependent Cugnon cross section (labeled SMD) is used in the present reactions. The value of E_{bal} is calculated

*Electronic address: ashuphysics@gmail.com

TABLE I: The mean values of percentage change in E_{bal} with impact parameter for $A_{TOT} = 40$ -240 with and without Coulomb potential.

System	Coul. ON		Coul. OFF	
	$b/b_{max} = 0.5$	$b/b_{max} = 0.75$	$b/b_{max} = 0.5$	$b/b_{max} = 0.75$
40	29.80	127.69	32.43	152.04
80	24.92	90.07	25.22	113.91
160	19.28	69.38	22.95	97.66
240	16.88	56.47	24.28	89.98

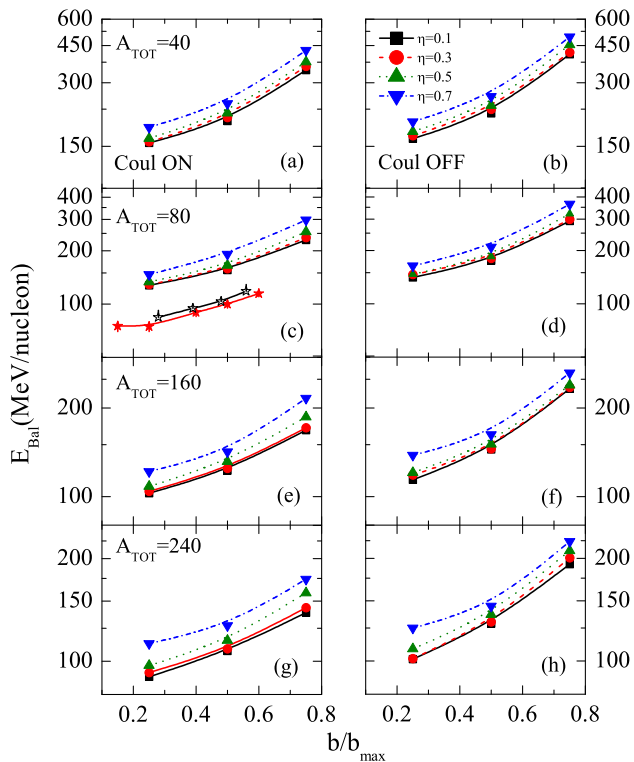


FIG. 1: (Color online) E_{bal} as a function of reduced impact parameter (a, c, e, g) with and (b, d, f, h) without Coulomb potential for different system masses. The results for different asymmetries $\eta = 0.1, 0.3, 0.5,$ and 0.7 are represented, respectively, by the solid squares, circles, triangles, and inverted triangles. Solid (open) stars in (c) represent data points of $^{40}\text{Ca} + ^{40}\text{Ca}$ ($^{40}\text{Ar} + ^{45}\text{Sc}$) and are taken from Ref. [14]. Lines are a guide for the eye.

using the *directed transverse momentum* $\langle P_x^{dir} \rangle$ and is defined in Ref. [6].

In Fig. 1, we display the impact parameter dependence of E_{bal} for different values of $\eta = 0.1, 0.3, 0.5,$ and 0.7 . The value of A_{TOT} is kept fixed as 40 [Figs 1(a) and 1(b)], 80 [Figs 1(c) and 1(d)], 160 [Figs 1(e) and 1(f)], and 240 [Figs 1(g) and 1(h)]. Various symbols are explained in the caption of the figure. From the figure it is clear that, for all mass ranges and colliding geometries, the value of E_{bal} increases with increase in η . This is because, with increase in η , the maximum

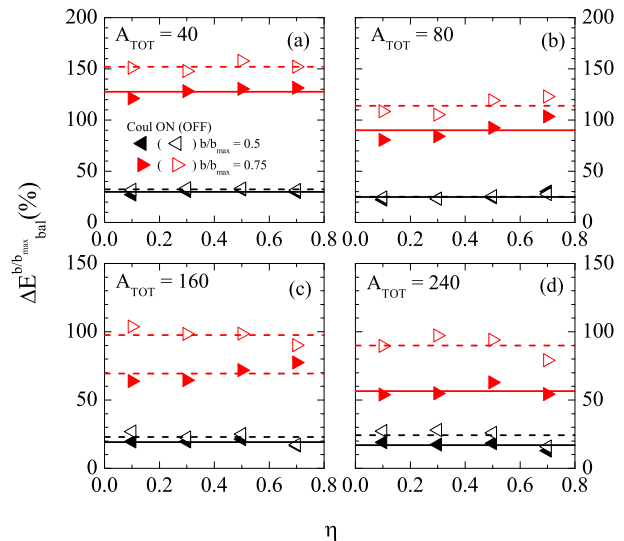


FIG. 2: (Color online) The percentage difference $\Delta E_{bal}^{b/b_{max}} (\%)$ as a function of η for different system masses. The results of the percentage difference for different colliding geometries $b/b_{max} = 0.5$ and 0.75 are represented, respectively, by the left- and right-pointing triangles. Open symbols represents results without Coulomb potential. Horizontal dotted lines represent the mean value of $\Delta E_{bal}^{b/b_{max}} (\%)$ for each b/b_{max} .

density and compression reached in the overlap zone decrease, which leads to the decrease in nn collisions. Furthermore, for all the mass ranges and η , the well-known trend of the increase of E_{bal} with impact parameter is seen. To precisely see the effect of mass asymmetry at different colliding geometries, results without Coulomb potential are also shown (labeled as Coul OFF). The results with Coulomb potential are labeled as Coul ON. It is clear from the figure that the effect of mass asymmetry on the E_{bal} increases with increase in impact parameter for all mass ranges. One can also see the enhancement in E_{bal} without Coulomb potential. This is caused by the decrease in the repulsive interactions. In Fig. 1(c), data points of $^{40}\text{Ca} + ^{40}\text{Ca}$ ($\eta=0$ and $A_{TOT} = 80$) and $^{40}\text{Ar} + ^{45}\text{Sc}$ ($\eta=0.06$ and $A_{TOT} = 85$) are also displayed [14]. The match with data is not seen because the SMD equation of state is used in the present study and E_{bal} is found to be highly sensitive toward the EOS and the

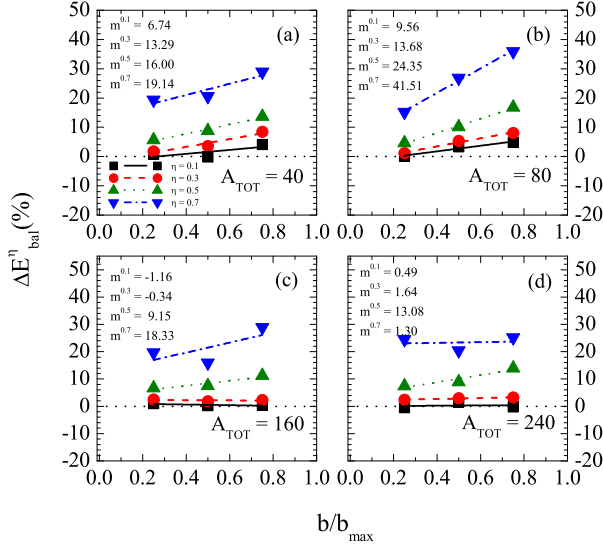


FIG. 3: (Color online) The percentage difference $\Delta E_{bal}^{\eta}(\%)$ as a function of b/b_{max} for different system masses. The results of the percentage difference for different asymmetries $\eta = 0.1, 0.3, 0.5,$ and 0.7 are represented, respectively, by the solid squares, circles, triangles, and inverted triangles. Lines are the linear fits ($\propto m \frac{b}{b_{max}}$); m values without errors are displayed. Results are with Coulomb potential.

nn cross section [1–3]. But the trend of variation with impact parameter is found to be the same.

In Fig. 2, we display the percentage change in balance energy $\Delta E_{bal}^{b/b_{max}}(\%)$, defined as $\Delta E_{bal}^{b/b_{max}}(\%) = ((E_{bal}^{b/b_{max} \neq 0.25} - E_{bal}^{b/b_{max} = 0.25}) / E_{bal}^{b/b_{max} = 0.25}) \times 100$ versus the asymmetry of the reaction. Lines represent the mean value of variation. Very interestingly, we see that for every fixed A_{TOT} , the effect of impact parameter variation is almost uniform throughout the asymmetry range. The values of mean variation are given in Table I. It is very clear from Table I that, that without Coulomb potential, the mean variation is greater compared to that with Coulomb potential. For the symmetric systems, it was found that the effect of the impact parameter on E_{bal} is greater for the lighter masses than for the heavier ones [13]. A similar trend was observed in the present study. We found that the mean variation decreases with increase in A_{TOT} . In total, it is clear from Fig. 2, that the effect of impact parameter variation is independent of η . In Fig. 3, we display the percentage difference $\Delta E_{bal}^{\eta}(\%)$ defined as $\Delta E_{bal}^{\eta}(\%) = ((E_{bal}^{\eta \neq 0} - E_{bal}^{\eta = 0}) / E_{bal}^{\eta = 0}) \times 100$ versus the reduced impact parameter (b/b_{max}). Lines are the linear fits ($\propto m \frac{b}{b_{max}}$). We see that the effect of the asymmetry variation increases with increase in the impact parameter for each mass range. It means that for peripheral collisions, the role of mass asymmetry is more as compared to central ones. This is due to the fact that with increase in impact parameter, the number of nn binary collisions decreases and the increase of mass asymmetry further adds the same effect.

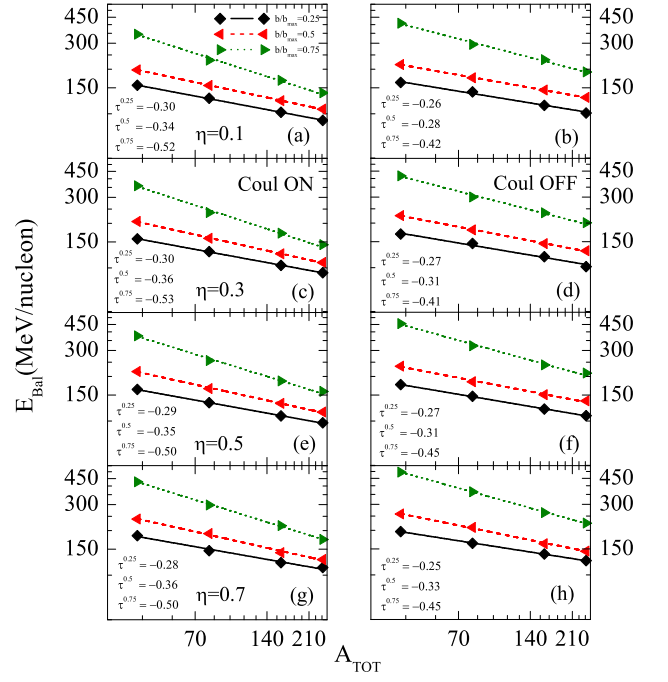


FIG. 4: (Color online) Left (right) panels display E_{bal} as a function of the combined mass of the system for different mass asymmetries (a, c, e, g) with and (b, d, f, h) without Coulomb potential. Solid diamonds, left-pointing triangles, and right-pointing triangles represents the calculations with $b/b_{max} = 0.25, 0.5,$ and $0.75,$ respectively. Lines are power-law fits $\propto A_{TOT}^{\tau}$; τ values without errors are displayed.

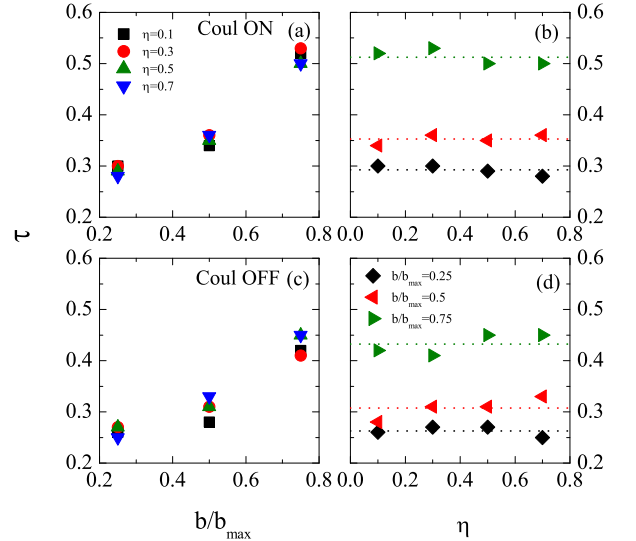


FIG. 5: (Color online) Values of τ as a function of (a, c) reduced impact parameter for $\eta = 0.1-0.7$ and (b, d) mass asymmetry for $b/b_{max} = 0.25-0.75$. τ values (a, b) with (c, d) without Coulomb potential. The horizontal dotted lines in (b) and (d) represent the mean value of τ for each b/b_{max} . Various symbols have the same meaning as in Figs. 1 and 4.

TABLE II: The values of $\tau^{0.25}$, $\tau^{0.5}$, and $\tau^{0.75}$ for $\eta = 0.1, 0.3, 0.5$, and 0.7 for calculations with and without Coulomb potential.

η	$\tau^{0.25}$		$\tau^{0.5}$		$\tau^{0.75}$	
	Coul. ON	Coul. OFF	Coul. ON	Coul. OFF	Coul. ON	Coul. OFF
0.1	-0.30	-0.26	-0.34	-0.28	-0.52	-0.42
0.3	-0.30	-0.27	-0.36	-0.31	-0.53	-0.41
0.5	-0.29	-0.27	-0.35	-0.31	-0.50	-0.45
0.7	-0.28	-0.25	-0.36	-0.33	-0.50	-0.45

In Fig. 4, we display E_{bal} as a function of A_{TOT} for $b/b_{max} = 0.25, 0.5$, and 0.75 , keeping η fixed as 0.1 [Figs. 4(a) and 4(b)], 0.3 [Figs. 4(c) and 4(d)], 0.5 [Figs. 4(e) and 4(f)], and 0.7 [Figs. 4(g) and 4(h)]. The results without Coulomb potential are also shown. Various symbols are explained in the caption of the figure. The lines are power-law fits ($\propto A^\tau$). From the figure, we see that E_{bal} follows the power-law behavior at all values of η and colliding geometry. The values of τ are given in Table II.

From Fig. 4, we see that for each value of η , as we go from central collisions to peripheral ones, E_{bal} increases. The increase is more for the lighter systems as compared to heavier ones. From the values of τ in Table II, we see that as we go from central to peripheral collisions, the value increases drastically for each η . For the symmetric systems, the values of τ are $-0.32, -0.34$, and -0.36 , respectively, at $b/b_{max} = 0.3, 0.45$, and 0.6 for the HMD^{40} (momentum dependent hard equation of state with constant cross section of 40mb) EOS [15]. Our results are for the SMD EOS and at $b/b_{max} = 0.25, 0.5$, and 0.75 , but the trend is still the same. The values of τ without Coulomb potential are less than the values with Coulomb potential, but the trend is the same. The variation of τ as a function of b/b_{max} and η is shown in Fig. 5.

In Fig. 5, we display the variation of τ as a function of b/b_{max} for $\eta = 0.1-0.7$ [Figs. 5(a) and 5(c)] and variation with respect to η for $b/b_{max} = 0.25-0.75$ [Figs. 5(b) and 5(d)]. Dotted lines in [Figs. 5(b) and 5(d)] represent the values of τ averaged over η . Symbols are explained in the caption of the figure. From the figure, it is clear that

τ increases with increase in impact parameter both with and without Coulomb potential. Very interestingly, the variation of τ with η is almost uniform as one goes from central to peripheral collisions. It means that the mass dependence of E_{bal} is independent of mass asymmetry at every colliding geometry. The values of τ averaged over η are 0.29 (0.26), 0.35 (0.30), and 0.51 (0.43), respectively, for $b/b_{max} = 0.25, 0.5$, and 0.75 with (without) Coulomb potential. The effect of Coulomb potential is greater for the heavier nuclei; therefore, the increase in E_{bal} is greater in the case of heavier nuclei as compared to lighter ones when the Coulomb potential is turned off. This leads to a decrease in value of τ when calculations are performed without Coulomb potential.

In summary, we studied the role of colliding geometry in the disappearance of flow as well as its mass dependence throughout the mass range $40-240$ for mass-asymmetric reactions with $\eta = 0.1-0.7$. Our results clearly demonstrate that the effect of mass asymmetry is more dominant at peripheral collisions than at central ones. Very interestingly, we found that the percentage change in E_{bal} with colliding geometry remains uniform throughout the mass-asymmetry range for every fixed system mass.

Author is thankful to Dr. Rajeev K. Puri for interesting and constructive discussions. This work is supported by a research grant from the Council of Scientific and Industrial Research (CSIR), government of India, vide Grant No. 09/135(0563)/2009-EMR-1.

-
- [1] K. G. R. Doss *et al.*, Phys. Rev. Lett. **57**, 302 (1986).
[2] H. A. Gustafsson *et al.*, Phys. Rev. Lett. **52**, 1590 (1984).
[3] W. Scheid, H. Müller, W. Greiner, Phys. Rev. Lett. **32**, 741 (1974).
[4] D. Krofcheck *et al.*, Phys. Rev. Lett. **63**, 2028 (1989).
[5] C. A. Ogilvie *et al.*, Phys. Rev. C **40**, 2592 (1989).
[6] S. Goyal and R. K. Puri, Nucl. Phys. **A853**, 164 (2011).
[7] J. Lukasik and W. Trautmann, in *Proceedings of the International Nuclear Physics Conference (INPC2007) (Tokyo, 2007)* (2008), Vol. 2, pp. 513-515, Nucl. Phys. **A805**, V (2008); B. Hong *et al.*, Phys. Rev. C **66**, 034901 (2000).
[8] Q. Pan and P. Danielewicz, Phys. Rev. Lett. **70**, 2062 (1993); J. Lukasik *et al.*, Phys. Lett. B **608**, 223 (2005).
[9] V. de la Mota, F. Sebillé, M. Farine, B. Remaud, P. Schuck, Phys. Rev. C **46**, 677 (1992); G. D. Westfall *et al.*, Phys. Rev. Lett. **71**, 1986 (1993); H. Zhou, Z. Li, Y. Zhuo, Phys. Rev. C **50**, R2664 (1994).
[10] D. J. Magestro, W. Bauer, G. D. Westfall, Phys. Rev. C **62**, 041603(R) (2000); A. D. Sood and R. K. Puri, Phys. Rev. C **69**, 054612 (2004); A. D. Sood and R. K. Puri, Phys. Rev. C **73**, 067602 (2006).
[11] A. D. Sood and R. K. Puri, Phys. Lett. B **594**, 260 (2004); A. D. Sood and R. K. Puri, Eur. Phys. J. A **30**, 571 (2006); S. Kumar, M. K. Sharma, R. K. Puri, K. P. Singh, and I. M. Govil, Phys. Rev. C **58**, 3494 (1998); A. D. Sood and R. K. Puri, Phys. Rev. C **70**, 034611 (2004); S. Gautam *et al.*, J. Phys. G: Nucl. Part. Phys. **37**, 085102 (2010); *ibid.* Phys. Rev. C **83**, 034606 (2011); V. Kaur, S. Kumar, and R. K. Puri, Phys. Lett. B **697**,

- 512 (2011).
- [12] J. P. Sullivan *et al.*, Phys. Lett. B **249**, 8 (1990); A. Buta *et al.*, Nucl. Phys. **A584**, 397 (1995); Z. Y. He *et al.*, Nucl. Phys. **A598**, 248 (1996); M. B. Tsang, G. F. Bertsch, W. G. Lynch, M. Tohyama, Phys. Rev. C **40**, 1685 (1989).
- [13] D. J. Magestro *et al.*, Phys. Rev. C **61**, 021602(R) (2000).
- [14] R. Pak *et al.*, Phys. Rev. C **53**, R1469 (1996); S. Soff, S. A. Bass, C. Hartnack, H. Stöcker, W. Greiner, Phys. Rev. C **51**, 3320 (1995).
- [15] R. Chugh and R. K. Puri, Phys. Rev. C **82**, 014603 (2010).
- [16] J. Aichelin, Phys. Rep. **202**, 233 (1991); S. Goyal and R. K. Puri, Phys. Rev. C **83**, 047601 (2011); Y. K. Vermani, S. Goyal, and R. K. Puri, Phys. Rev. C **79**, 064613 (2009); Y. K. Vermani *et al.*, J. Phys. G: Nucl. Part. Phys. **37**, 015105 (2010); Y. K. Vermani and R. K. Puri, J. Phys. G: Nucl. Part. Phys. **36**, 105103 (2009).